

論文

반경방향의 모서리 균열을 갖고 내면이 경사기능재료(FGM)로 코팅된
두꺼운 실린더의 결보기 파괴인성해석

알리 모하마드 압사*, 라셀*, 송정일**

Analysis of Apparent Fracture Toughness of a Thick-Walled Cylinder with an FGM
Coating at the Inner Surface Containing a Radial Edge Crack

A. M. Afsar*, S. M. Rasel* and J. I. Song**

ABSTRACT

This study analyzes the apparent fracture toughness of a thick-walled cylinder with a functionally graded material (FGM) coating at the inner surface of the cylinder. The cylinder is assumed to have a single radial edge crack emanating from its inner surface. The crack surfaces and the inner surface of the cylinder are subjected to an internal pressure. The incompatible eigenstrain developed in the cylinder due to nonuniform coefficient of thermal expansion as a result of cooling from sintering temperature is taken into account. Based on a method of evaluating stress intensity factor introduced in our previous study, an approach is developed to calculate apparent fracture toughness. The approach is demonstrated for a cylinder with a TiC/Al₂O₃ FGM coating and some numerical results of apparent fracture toughness are presented graphically. The effects of material distribution profile, cylinder wall thickness, application temperature, and coating thickness on the apparent fracture toughness are investigated in details. It is found that all of these factors play an important role in controlling the apparent fracture toughness of the cylinder.

초 록

본 연구는 실린더 내부가 경사기능재료로 코팅된 두꺼운 벽을 가진 실린더의 결보기 파괴인성치를 해석한 것이다. 실린더는 내부로부터 반경방향의 단일 모서리 균열이 내재되어 있으며, 균열면과 내면에는 내압을 받고 있는 것으로 가정하였다. 소결온도로부터 냉각 결과 균일한 열팽창계수로 인해 실린더에는 비적합 고유스트레인이 생성되었다. 기존의 연구에서 소개된 응력확대계수 평가법에 기초해 결보기 파괴인성치를 계산하였다. 본 연구에서는 TiC/Al₂O₃ FGM코팅된 실린더를 사용하였고 결보기 파괴인성치의 수치적인 결과를 도식화하였다. 재료분포프로파일, 실린더 벽 두께, 적용온도와 코팅두께 등이 결보기 파괴인치에 미치는 영향이 상세히 조사되었으며, 이러한 모든 인자는 실린더의 결보기 파괴인성치를 조절하는데 중요한 역할을 하는 것으로 밝혀졌다.

Key Words : 경사기능재료(Functionally graded materials), 두꺼운 벽 실린더(Thick-walled cylinder), 응력확대계수(Stress intensity factor), 결보기파괴인성치(Apparent fracture toughness), 모서리 균열(Edge cracks), 고유스트레인(Eigenstrain)

1. Introduction

Functionally graded materials (FGMs) consist of two or more distinct material phases such as different ceramics or

* Dept. of Mechanical Engineering, Changwon National University

**+ Dept. of Mechanical Engineering, Changwon National University, Correspondence(E-mail:jisong@changwon.ac.kr)

ceramics and metals. However, the distinguishing feature of these materials is that the volume fractions of the constituent materials continuously vary with space variables. This makes the FGMs different from homogeneous materials and conventional composite materials [1, 2]. Because of the continuously varying material distribution, both the mechanical and thermal properties of FGMs become nonhomogeneous. In addition, the microstructures of these materials are also dependent on the space variables. The concept of FGMs was introduced in 1984 by Japanese scientists in Sendai area [2] and the original purpose of these unique materials was to develop superheat-resistant materials for propulsion systems and airframes of spacecraft.

From a mechanics viewpoint, the material property grading provides numerous advantages, such as improved bonding strength, toughness, wear and corrosion resistance, and reduced residual and thermal stresses. Some typical applications include thermal barrier coatings of high temperature components in gas turbines, surface hardening for tribological protection and graded interlayers used in multilayered microelectronic and optoelectronic components [1-3].

Because of their outstanding advantages, FGMs have now received wide attention towards the development of new potential structural applications. Obviously, design of all structural elements requires the consideration of their fracture characteristics to ensure structural integrity in service. Although the absence of sharp interfaces in FGMs does largely reduce material property mismatch, cracks may occur when they are subjected to external loadings [1, 2]. Very often the process begins with the formation of microcracks at locations of corrosion pits, surface flaws, or severe stress concentrations. Generally, a number of microcracks coalesce and form a local dominant crack, which would then propagate subcritically under cyclic or sustained loading. The loads or stresses acting on the medium may be mechanically or thermally induced. There are also uncertainties arising from voids and defects that are introduced in FGMs during manufacturing. Even a small quantity of mechanical imperfections can cause a marked influence on their fracture strength. Therefore, the study of the fracture characteristics of these materials appears to be an utmost necessary to understand, quantify, and improve their toughness.

However, the nonhomogeneous properties of FGMs make their analytical fracture studies very complicated due to mathematical limitation. To overcome this problem and make the problem tractable, customarily, the nonhomogeneous

material properties of FGMs are simulated to vary following some assumed functions, such as exponential [4-8] and power functions [9,10]. However, the assumed functions for the material properties are not always adequate to understand the actual fracture characteristics of FGMs. In particular, the specific assumed functional forms of material properties cannot be used in inverse problems in which a desired characteristic under a given mechanical or thermal loading is assumed in FGMs and the corresponding optimum material distribution is evaluated. Zuiker [11] pointed out that the assumed material property distributions are not physically realizable for certain material distribution profiles which may be obtained by the inverse problems. To get rid of this difficulty, an approximation method was developed by Sekine and Afsar [12] and Afsar and Sekine [13] for evaluating stress intensity factor for a single edge crack and periodic edge cracks, respectively, in a semi-infinite FGM medium. The outstanding advantage of the method is that it can deal with any arbitrary distribution of material properties. Thus, it can be readily applied to the inverse problem of evaluating material distributions. Another indispensable issue to be considered while dealing with the fracture of FGMs is the incompatible eigenstrain [14]. Eigenstrain is a generic name of such nonelastic strains as thermal expansion, phase transformation, initial strains, plastic strains, and misfit strains. The incompatibility of these eigenstrains results in eigenstress, which is the self-equilibrated internal stress and has significant effects on the fracture strength of FGMs. The eigenstrain may be induced in a material due to various reasons. In FGMs, it is induced due to non-uniform coefficient of thermal expansion (CTE) when FGMs are cooled from sintering temperature. The approximation method developed by Sekine and Afsar [12] and Afsar and Sekine [13] considered this eigenstrain.

The concept of the above approximation method was extended for a single radial edge crack in a thick-walled FGM cylinder [15] and a circular hole with an FGM coating in an infinite medium [16]. More recently, the method was generalized for two diametrically opposed edge cracks in a thick-walled FGM cylinder to evaluate stress intensity factors [17] by direct method and material distribution realizing desired fracture characteristics by inverse method [18]. Based on the generalized method of stress intensity factors [17], another approach [19] is developed for analyzing apparent fracture toughness of a thick-walled FGM cylinder with two diametrically opposed edge cracks. However, in practice, it is not feasible to manufacture a thick-walled cylinder with

graded material distribution throughout the entire wall thickness because of the manufacturing limitation as well as the huge cost involvement. Also, from engineering points of view, the entire cylinder wall thickness with graded material distribution is not important in order to meet requirements of an application. Only a thin FGM coating can suffice the requirements of an application and is more feasible from technical points of view.

Thus, the present study focuses on a thin FGM coating at the inner surface of a thick-walled cylinder for the analysis of apparent fracture toughness against a single radial edge crack emanating from the inner surface of the cylinder. Taking into account the incompatible eigenstrain developed in the cylinder and based on the method of evaluating stress intensity factor developed in an earlier study [17], an approach of evaluating apparent fracture toughness is introduced. The effects of material distribution, cylinder wall thickness, application temperature, and coating thickness on the apparent fracture toughness are investigated in details using the developed method.

2. Effective Properties of FGMs

The effective properties of FGMs can be determined by using mixture rule formulas. It is noted that the mixture rule formulas developed for the conventional composites cannot be used for FGMs as the volume fractions of the constituents and the resulting microstructures are varying continuously in an FGM. Therefore, a special care should be taken into account while deriving a mixture rule formula for the effective properties of FGMs so that it can be applicable for the entire range of variation of volume fractions. In this study, the mixture rule formula developed by Nan et al. [20] is used for the determination of the effective properties. This mixture rule formula is valid for any value of the volume fractions of the constituent materials ranging from 0 to 1. For the two constituent materials *A* and *B*, it is given by

$$V_A \frac{K_A - K}{3K_A + 4\mu} + V_B \frac{K_B - K}{3K_B + 4\mu} = 0 \quad (1a)$$

$$V_A \frac{\mu_A - \mu}{\mu_A + Y} + V_B \frac{\mu_B - \mu}{\mu_B + Y} = 0 \quad (1b)$$

$$\alpha = V_A \alpha_A \frac{K_A(3K + 4\mu)}{K(3K_A + 4\mu)} + V_B \alpha_B \frac{K_B(3K + 4\mu)}{K(3K_B + 4\mu)} \quad (1c)$$

$$Y = \frac{\mu(9K + 8\mu)}{(6K + 12\mu)} \quad (1d)$$

$$E = \frac{9K\mu}{(3K + \mu)} \quad (1e)$$

where *V* is the volume fraction, *K* is the bulk modulus, *E* is the Young's modulus and μ is the shear modulus of elasticity, α is the coefficient of thermal expansion. The subscripts *A* and *B* denote the respective properties of the constituent materials, and the non-subscripted variables are used to denote the effective properties of the FGM.

3. Apparent Fracture Toughness of a Thick-Walled Cylinder with an FGM Coating

As pointed out earlier, an incompatible eigenstrain is developed in an FGM body, which causes eigenstress. Therefore, the effective or actual crack driving force in an FGM body is the resultant effect of the eigenstress and the applied load. However, the eigenstress is the inherent phenomenon of an FGM body. It plays the role behind the scenario. Thus, apparently it seems that a crack in an FGM body propagates due to the applied load only. Therefore, when only the applied load is taken into account to evaluate stress intensity factor of an FGM body, its critical value gives the apparent fracture toughness of the FGM body. A thick-walled cylinder with an FGM coating at its inner surface also experiences an eigenstress. Therefore, if only the internal applied pressure is considered to evaluate the stress intensity factor of a crack in such a cylinder, its critical value gives the apparent fracture toughness of the cylinder. Thus, for a single radial edge crack emanating from the inner surface of the cylinder with an FGM coating at its inner surface, the apparent fracture toughness, K_{IC}^a , is defined as

$$K_{IC}^a = F_I p_c \sqrt{\pi l} \quad (2)$$

where *F_I* is the geometric factor whose value is available in literatures [21], *p_c* is the critical value of applied internal pressure, and *l* is the crack length.

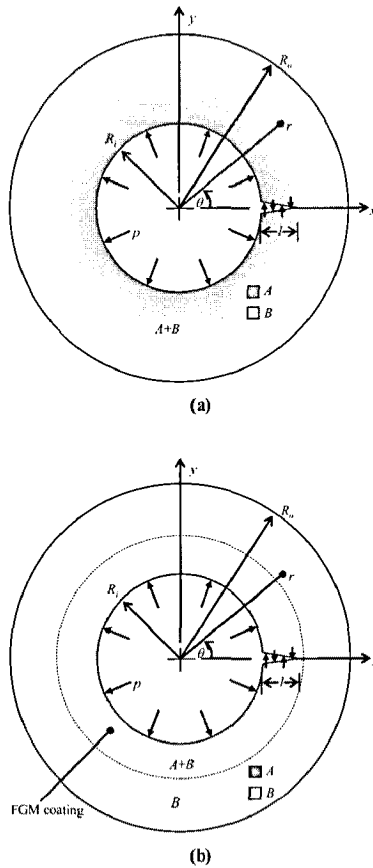


Fig. 1 Analytical model of (a) an FGM thick-walled cylinder, (b) a thick-walled cylinder with an FGM coating at its inner surface.

4. Intrinsic Fracture Toughness of a Thick-Walled Cylinder with an FGM Coating

The intrinsic fracture toughness of FGMs, on the other hand, represents the effective or actual crack driving force which corresponds to the resultant effect of the eigenstress and applied load. It is independent of the geometry of an FGM body, crack orientation and geometry, and eigenstress. It is absolutely a material property and its value at a point of FGM solely depends on the material composition of that point. Therefore, the intrinsic fracture toughness of FGMs can be determined from their effective properties. If a material *A* is dispersed in a matrix material *B* and forms an *A/B* FGM, the intrinsic fracture toughness, K_c , of the FGM can be determined from [22]

$$K_c = \frac{E}{E_B} K_c^B \quad (3)$$

where E is the Young's modulus of FGMs and E_B and K_c^B are the Young's modulus and fracture toughness of the base material *B*, respectively. The effective Young's modulus E of the FGM is determined using the mixture rule formula given by Eq. (1).

5. Stress Intensity Factor

The approach presented in this study for evaluating apparent fracture toughness is based on the method of evaluating stress intensity factors developed by Afsar and Sekine [15]. Thus, this section is intended to give a concise description of the method of evaluating stress intensity factor [15]. Figure 1(a) shows a thick-walled FGM cylinder with a radial edge crack at its inner surface. The inner radius, outer radius, and the length of the crack are denoted by R_i , R_o , and l , respectively. The FGM cylinder is assumed to be composed of two materials *A* and *B*, the volume fractions of which are represented by V_A and V_B , respectively. The black color represents the material *A* while the white color represents the material *B*. The material distribution varies in radial direction only. Therefore, all the material properties are the functions of r only. Due to the nonuniform coefficient of thermal expansion, an incompatible eigenstrain [14] is developed in the cylinder when it is cooled from sintering temperature. This incompatible eigenstrain causes an eigenstress [14] which plays an important role to characterize the fracture behavior of the FGM cylinder. Thus, the incompatible eigenstrain is taken into account and is given by

$$\varepsilon^*(r) = -\Delta T \alpha(r) \quad (4)$$

where α is the coefficient of thermal expansion and ΔT is the difference between sintering and application temperatures.

The cylinder is subjected to an internal pressure p . Thus, the effective crack driving force is produced due to the combined effect of the internal pressure p and the eigenstress associated with the incompatible eigenstrain. By considering an additional eigenstrain called equivalent eigenstrain [15], the FGM cylinder is replaced by a homogeneous cylinder of

material B only. Then using the distributed dislocation technique to represent the cracks, the problem of evaluating stress intensity factor for this model of the cylinder with a radial edge crack is reduced to the solution of the following system of simultaneous linear algebraic equation [15]:

$$\frac{2\mu_B}{\kappa_B + 1} \left[\sum_{\xi=1}^N \phi(S_\xi)(1+S_\xi) \left\{ \frac{1}{T_\eta - S_\xi} + G_1(T_\eta) + G_2(T_\eta, S_\xi) \right\} \right] = -\frac{2N+1}{2} [\sigma_o^h(T_\eta) + p] \quad (5)$$

where μ_B is the shear modulus of material B, κ_B is the Kolosov's constant of material B, and $\phi(S_\xi)$ is the density function of distributed dislocations. The integration and collocation points S_ξ and T_η are, respectively, given by

$$S_\xi = \cos\left(\frac{2\xi-1}{2N+1}\pi\right); \quad \xi = 1, 2, \dots, N \quad (6a)$$

$$T_\eta = \cos\left(\frac{2\eta}{2N+1}\right); \quad \eta = 1, 2, \dots, N \quad (6b)$$

The functions $G_1(T_\eta)$, $G_2(T_\eta, S_\xi)$ and the expression of the circumferential stress component $\sigma_o^h(T_\eta)$ are available in our previous study [15]. The expression of circumferential stress component $\sigma_o^h(T_\eta)$ has two parts. One part is associated with the internal pressure p and the other part is the function of eigenstrains.

The solution of Eq. (5) gives the discrete values of $\phi(S_\xi)$ behind the crack tip. However, the determination of stress the intensity factor requires the value of $\phi(S_\xi)$ at the crack tip which is determined using the values of $\phi(S_\xi)$ behind the crack tip in Krenk's interpolation formula given by

$$\phi(+1) = \frac{2}{2N+1} \sum_{\xi=1}^N \frac{\sin\left(\frac{2\xi-1}{2N+1}N\pi\right)}{\tan\left(\frac{2\xi-1}{2N+1}\frac{\pi}{2}\right)} \phi(S_\xi) \quad (7)$$

The stress intensity factor is then determined from

$$K_I = \frac{2\mu_B}{\kappa_B + 1} \sqrt{2\pi l} \phi(+1) \quad (8)$$

It is noted that the stress intensity factor formulations discussed above are derived for the cylinder whose entire wall consists of FGM, i.e., the entire wall has the variation of material distribution. The same formulations can be used for a thick-walled cylinder with an FGM coating at the inner surface only as shown in Fig. 1(b). In this case, the material distribution varies only over the coating region (denoted by region $A+B$) while it remains uniform over the other part of the wall cylinder (denoted by region B). To apply the above formulations of stress intensity factor to the latter case (Fig. 1(b)), one only requires to assume variable properties in the coating region and uniform properties outside the coating region while rest of the procedure is the same.

6. Approach of Evaluating Apparent Fracture Toughness

In this section, an approach is introduced to evaluate apparent fracture toughness using the formulations of stress intensity factors discussed in the preceding section. Equations (5) to (8) determine the stress intensity factor due to the combined effect of the eigenstrain and applied internal pressure. Therefore, the critical value of the stress intensity factor at the crack tip determined from Eqs. (5) to (8) must be equal to the intrinsic fracture toughness, determined from Eq. (3), of the point of crack tip position. It is noted that the right hand side of Eq. (5) is the function of eigenstrains and applied internal pressure. Therefore, for a prescribed material distribution and crack length, this equation can be solved in terms of unknown internal pressure p in the form of

$$K_I = k_e + k_p p \quad (9)$$

where k_e is the stress intensity factor associated with the eigenstrains and k_p is the factor associated with the coefficient of p in Eq. (5). Then, Eqs. (3) and (9) are equated to determine the critical value of the internal pressure p_c corresponding to a given crack length. Note that the right hand side of Eq. (3) is known as the material

distribution is already prescribed from which E can be determined by mixture rule formula given by Eq. (1). The critical value of the internal pressure p_c is then used in Eq. (2) to determine the apparent fracture toughness of the point of the crack tip position. Equations (5) to (8) are solved by varying the crack length and the apparent fracture toughness is determined at the position of crack tip following the above procedure.

7. Results and Discussion

In this section, an Al_2O_3 thick-walled cylinder with a $\text{TiC}/\text{Al}_2\text{O}_3$ FGM coating at its inner surface is considered to demonstrate the approach of evaluating apparent fracture toughness. The materials A and B correspond to TiC and Al_2O_3 , respectively, whose properties are shown in Table 1. The approach can be applied to any combination of materials. However, the TiC and Al_2O_3 have been chosen here merely as an example to generate some numerical results of apparent fracture toughness. The simultaneous equations represented by Eq. (5) are solved by Gauss elimination method where the parameter N is taken as 50 which ensures well the convergence of the results.

As mentioned earlier, the present approach of evaluating apparent fracture toughness is based on the method of evaluating stress intensity factor developed by Afsar and Sekine [15]. Therefore, the validity of the method of evaluating stress intensity factor [15] guarantees the validity of the present approach of evaluating apparent fracture toughness. Note that the validity of the method of evaluating stress intensity factor has already been verified in Ref. [15], which, thus, guarantees the validity of the present approach of evaluating apparent fracture toughness. So, the verification of the present approach is irrelevant and abandoned in this study to avoid repeating occurrence.

Table 1 Material properties of TiC and Al_2O_3

Material	Young's Modulus (GPa)	Shear Modulus (GPa)	Poisson's Ratio	CTE ($^{\circ}\text{C}^{-1}$)	Fracture Toughness ($\text{MPa m}^{1/2}$)
TiC	462	194.12	0.19	7.4×10^{-6}	4.1
Al_2O_3	380	150.79	0.26	8.0×10^{-6}	3.5

The approach developed in the study is capable of evaluating apparent fracture toughness for both the cases of

an FGM coating at the inner surface of a thick-walled cylinder and a thick-walled cylinder with its entire wall thickness composed of FGM. The second case is referred to FGM cylinder. First, the results are presented for the FGM cylinder to examine the effects of material distribution, cylinder wall thickness, and application temperature on the apparent fracture toughness. Second, the effect of coating thickness is discussed to understand the fracture characteristics of the cylinder with an FGM coating at its inner surface.

Figure 2 shows four different prescribed material distributions over the entire wall thickness of the cylinder. The four distributions are Linear, Parabolic-1, Parabolic-2, and Uniform distributions. For these prescribed material distributions, the corresponding normalized apparent fracture toughness is presented in Fig. 3. The apparent fracture toughness K_{IC}^a is normalized by dividing it with the intrinsic fracture toughness K_{IC}^0 of Al_2O_3 . The difference between sintering and room temperatures is considered as 1000°C and the ratio of the cylinder outer to inner radii R_o/R_i is taken as 2.5. For all the cases of material distributions, the apparent fracture toughness initially increases over certain inner region of the cylinder wall. Then it decreases over rest of the wall thickness. This type of fracture characteristic is desirable as it ensures the protection of catastrophic failure. Once the crack starts to propagate under a certain pressure, it immediately stops propagating as the region ahead of the crack tip has a higher toughness. For its further propagation, the internal pressure should be increased. The maximum peak value of apparent fracture toughness is obtained for the uniform material distribution. However, the uniform distribution is not recommended as it has a sharp interface that causes the problem of delamination. Among other three distributions, it is noted that the parabolic 1 distribution gives the maximum value of apparent fracture toughness over the inner part of the cylinder wall. It is also noted that the apparent fracture toughness for all the material distributions has the value which is significantly higher than the intrinsic fracture toughness K_{IC}^0 of the base material Al_2O_3 over most of the cylinder wall except those at and near the inner and outer surfaces of the cylinder.

The effect of cylinder wall thickness on the apparent fracture toughness is exhibited in Fig. 4. The results correspond to the linear material distribution of Fig. 2 and $\Delta T = 1000^{\circ}\text{C}$. It is found that, for the same type of material distribution, apparent fracture toughness improves with the increase of the wall thickness.

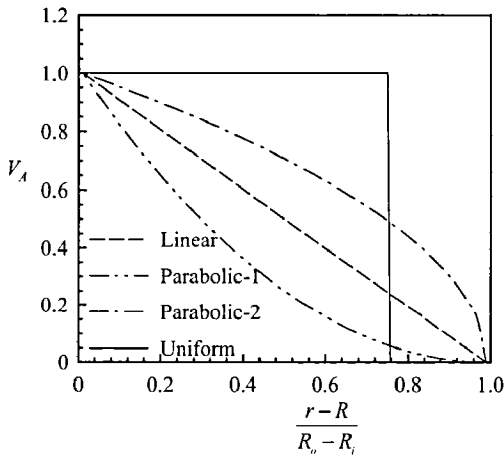


Fig. 2 Material distribution of TiC in radial direction.

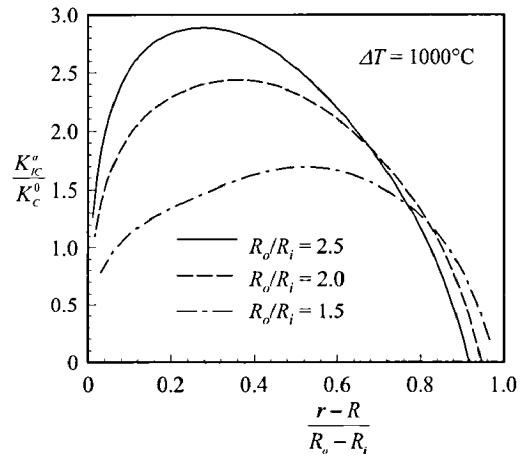


Fig. 4 Effect of wall thickness on normalized apparent fracture toughness.

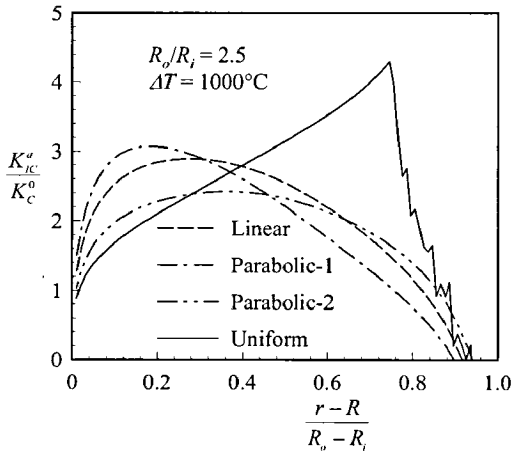


Fig. 3 Effect of material distribution on normalized apparent fracture toughness.

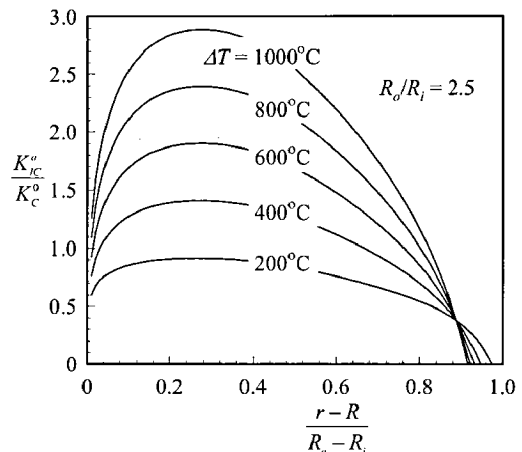


Fig. 5 Effect of application temperature on normalized apparent fracture toughness.

For linear material distribution and $R_o/R_i = 2.5$, apparent fracture toughness is shown in Fig. 5 as a function of application temperature. The parameter ΔT refers to the difference between the sintering and application temperature. Thus, a lower value of ΔT indicates the higher application temperature. It is evident from Fig. 5 that the cylinder has better fracture resistance at low application temperature. It is also noted that the apparent fracture toughness is worse than the intrinsic fracture toughness of the base material Al_2O_3 if the value of the parameter ΔT falls below $400^\circ C$.

To investigate the effect of the FGM coating thickness on the apparent fracture toughness, FGM coatings of various thicknesses are considered as shown in Fig. 6. The coating thicknesses are expressed in terms of the percent of the

cylinder wall thickness. In all the cases, the volume fraction of TiC varies linearly from 1.0 to zero over the coating thickness. Outside the FGM coating, the cylinder wall is composed of Al_2O_3 only. For each coating thickness, the corresponding apparent fracture toughness is shown in Fig. 7. The results correspond to $\Delta T=1000^\circ C$ and $R_o/R_i = 2.5$. For any coating thickness, the apparent fracture toughness rises to a peak value with radial distance over the inner region of the cylinder wall. Then it starts decreasing over rest of the region of the wall. The position of the peak value of the apparent fracture toughness shifts towards the outer surface as the coating thickness increases. Further, the peak value of apparent fracture toughness increases with the increase of the coating thickness until the coating thickness

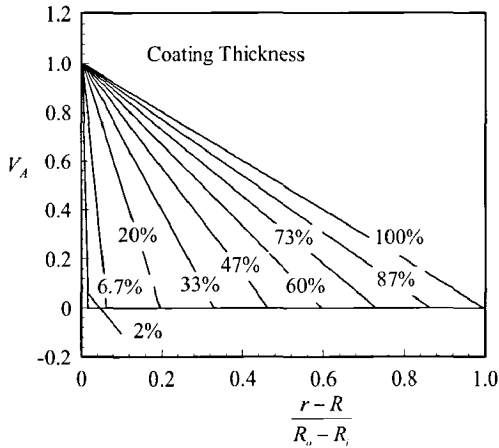


Fig. 6 Coating thickness and material distribution of TiC.

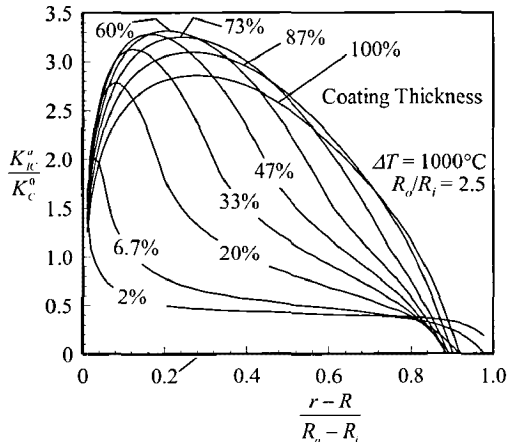


Fig. 7 Effect of coating thickness on normalized apparent fracture toughness.

is 60% of the cylinder wall thickness. After this value of the coating thickness, the apparent fracture toughness start degrading as the coating thickness further increases.

8. Conclusions

An approach is introduced to evaluate apparent fracture toughness of a thick-walled cylinder with an FGM coating at its inner surface and containing a single radial edge crack emanating from the inner surface of the cylinder. The effect of eigenstrain developed in the cylinder as a result of cooling from sintering temperature due to nonuniform coefficient of thermal expansion is taken into account. The approach is demonstrated for a TiC/Al₂O₃ FGM coating at the inner surface of an Al₂O₃ thick-walled cylinder. The

effects of the material distribution, cylinder wall thickness, application temperature, and coating thickness on the apparent fracture toughness are investigated. It is found that all of these parameters play an important role in controlling the apparent fracture toughness of the cylinder. Thus, these parameters should be properly controlled to control the apparent fracture toughness in designing with a thick-walled cylinder with an FGM coating its inner surface.

Acknowledgement

This work was supported by the Korea Research Foundation (KRF) grant funded by the Korea government (MEST) (No. KRF 2009-0076450). The authors would also like to acknowledge the partial support from the Second stage of Brain Korea 21 Project Corps.

References

- 1) Yamanouchi, M., Koizumi, M., Hirai T., and Shiota I., "Proceedings of the First International Symposium on Functionally Gradient Materials," Sendai, Japan, 1990.
- 2) Holt, J.B., Koizumi M., Hirai T., and Munir Z.A., *Ceramic Transactions: Functionally Gradient Materials*, Vol. 34, The American Ceramic Society, Westerville, OH, 1993.
- 3) Ilschner B. and Cherradi N., "Proceedings of the Third International Symposium on Structural and Functional Gradient Materials," Presses Polytechniques et Universitaires Romands, Lausanne, Switzerland, 1994.
- 4) Chen Y.F. and Erdogan F., "The Interface Crack Problem for a Nonhomogeneous Coatings Bonded to a Homogeneous Substrate," *Journal of the Mechanics and Physics of Solids*, Vol. 44, 1996, pp. 771-787.
- 5) Gu P. and Asaro R.J., "Cracks in Functionally Graded Materials," *International Journal of Solids and Structures*, Vol. 34, 1997, pp. 1-17.
- 6) Ozturk M. and Erdogan F., "An Axisymmetric Crack in Bonded Materials with a Nonhomogeneous Interfacial Zone under Torsion," *ASME Journal of Applied Mechanics*, Vol. 62, 1995, pp. 116-125.
- 7) Ozturk M. and Erdogan F., "Axisymmetric Crack Problem in Bonded Materials with a Graded Interfacial Region," *International Journal of Solids and Structures*, Vol. 33, 1996, pp. 193-219.
- 8) Choi H.J., "Bonded Dissimilar Strips with a Crack

- Perpendicular to the Functionally Graded Interface," *International Journal of Solids and Structures*, Vol. 33, 1996, pp. 4101-4117.
- 9) Bao G. and Wang L., "Multiple Cracking in Functionally Graded Ceramic/Metal Coatings," *International Journal of Solids and Structures*, Vol. 32, 1995, pp. 2853-2871.
- 10) Hassan H.A.Z., "Torsion of a Nonhomogeneous Infinite Elastic Cylinder Slackened by a Circular Cut," *Journal of Engineering Mathematics*, Vol. 30, 1996, pp. 547-555.
- 11) Zuiker J.R., "Functionally Graded Materials: Choice of Micromechanics Model and Limitations in Property Variation," *Composites Engineering*, Vol. 5, 1995, pp. 807-819.
- 12) Sekine H. and Afsar A.M., "Composition Profile for Improving the Brittle Fracture Characteristics in Semi-Infinite Functionally Graded Materials," *JSME International Journal*, Series A, Vol. 42, 1999, pp. 592-600.
- 13) Afsar A.M. and Sekine H., "Crack Spacing Effect on the Brittle Fracture Characteristics of Semi-Infinite Functionally Graded Materials with Periodic Edge Cracks," *International Journal of Fracture*, Vol. 102, 2000, pp. L61-L66.
- 14) Mura T., *Micromechanics of Defects in Solids: Mechanics of Elastic and Inelastic Solids*, Kluwer Academic Publishers, Dordrecht, The Netherlands, 1987.
- 15) Afsar A.M., and Sekine H., "Optimum Material Distributions for Prescribed Apparent Fracture Toughness in Thick-Walled FGM Circular Pipes," *International Journal of Pressure Vessels and Piping*, Vol. 78, 2001, pp. 471-484.
- 16) Afsar A.M. and Sekine H., "Inverse Problems of Material Distributions for Prescribed Apparent Fracture Toughness in FGM Coatings Around a Circular Hole in Infinite Elastic Media," *Composites Science and Technology*, Vol. 62, 2002, pp. 1063-1077.
- 17) Afsar A.M. and Anisuzzaman M., "Stress Intensity Factors of Two Diametrically Opposed Edge Cracks in a Thick-Walled Functionally Graded Material Cylinder," *Engineering Fracture Mechanics*, Vol. 74, 2007, pp. 1617-1636.
- 18) Afsar A.M., Anisuzzaman M., and Song J.I., "Inverse Problem of Material Distribution for Desired Fracture Characteristics in a Thick-Walled Functionally Graded Material Cylinder with Two Diametrically-Opposed Edge Cracks," *Engineering Fracture Mechanics*, Vol. 76, 2009, pp. 845-855.
- 19) Afsar A.M. and Song J.I., "Analysis of Apparent Fracture Toughness of a Thick-Walled FGM Cylinder with Two Diametrically Opposed Edge Cracks," *Fracture and Fatigue of Engineering Materials and Structures*, in press.
- 20) Nan C.W., Yuan R.Z., and Zhang L.M., *The Physics of Metal/Ceramic Functionally Gradient Materials*, Ceramic Transaction: Functionally Gradient Materials, Holt J.B. et al (ed), Vol. 34, American Ceramic Society, Westerville, Oh, 1993, pp. 75-82.
- 21) Bowie O.L. and Freese C.E., "Elastic Analysis for a Radial Crack in a Circular Ring," *Engineering Fracture Mechanics*, Vol. 4, 1972, pp. 315-321.
- 22) Nair S.V., "Crack-Wake Debonding and Toughness in Fiber-or Whisker-Reinforced Brittle-Matrix Composites," *Journal of American Ceramic Society*, Vol. 73, 1990, pp. 2839-2847.